nature reviews materials

https://doi.org/10.1038/s41578-024-00754-2

Perspective

Check for updates

The amorphous state as a frontier in computational materials design

Yuanbin Liu[1], Ata Madanchi[2], Andy S. Anker[1,3], Lena Simine[2] ✉ & Volker L. Deringer[1] ✉

Abstract

One of the grand challenges in the physical sciences is to 'design' a material before it is ever synthesized. There has been fast progress in predicting new solid-state compounds with the help of quantum-mechanical computations and supervised machine learning, and yet such progress has largely been limited to materials with ordered crystal structures. In this Perspective, we argue that the computational design of entirely non-crystalline, amorphous solids is an emerging and rewarding frontier in materials research. We show how recent advances in computational modelling and artificial intelligence can provide the previously missing links among atomic-scale structure, microscopic properties and macroscopic functionality of amorphous solids. Accordingly, we argue that the combination of physics-based modelling and artificial intelligence is now bringing amorphous functional materials 'by design' within reach. We discuss new implications for laboratory synthesis, and we outline our vision for the development of the field in the years ahead.

Sections

Introduction

Amorphous materials for emerging technologies

Realistic models of amorphous structures

Connecting structure and properties

Towards computational design

Outlook

[1]Department of Chemistry, University of Oxford, Oxford, UK. [2]Department of Chemistry, McGill University, Montreal, Québec, Canada. [3]Department of Energy Conversion and Storage, Technical University of Denmark, Kongens Lyngby, Copenhagen, Denmark. ✉e-mail: Lena.Simine@McGill.CA; volker.deringer@chem.ox.ac.uk

Introduction

New technologies depend crucially on scientific research to find materials with suitable properties: solar-cell absorbers for clean energy[1], electronic materials for brain-like computing[2–4] or biocompatible sensors for health care[5–7] are just a few examples. Although many materials have ordered crystalline structures, others are disordered: there is static and dynamic disorder in crystalline materials[8,9], and there are fully amorphous (non-crystalline) solids. Traditionally, amorphous materials have been of fundamental interest because of their complex medium-range structural order[10–12] and network topology[13,14]. Today, they are rapidly gaining importance in many commercially relevant fields such as optoelectronics, catalysis and batteries[15–17], sometimes even outperforming their crystalline counterparts. For example, amorphous boron nitride has been explored for use in high-performance electronics owing to its low dielectric constant, which is less than half of that of crystalline hexagonal boron nitride at 1 MHz (ref. 18). Another case is amorphous $LiFeSO_4F$, a high-capacity battery electrode material: its disordered structure is inherently defect-tolerant, enabling higher capacities and superior charge–discharge cycle stability compared with the crystalline polymorphs[19].

The space of all possible materials is immeasurably large, and therefore the computational discovery of new and useful materials is an outstanding challenge in the physical sciences. For crystalline solids, there has been much progress in computational materials discovery and design[20–25], enabled by 'first-principles' quantum-mechanical methods that have typically been based on density-functional theory (DFT). More recent studies have shown how the search for crystalline materials can be accelerated even further by using machine-learning (ML) methods[26,27]. For example, a DFT-trained interatomic potential model enabled the prediction of more than 2 million potential new crystalline materials, with 381,000 being computationally identified as thermodynamically stable[26]. Beyond the virtual screening in that study, autonomous laboratories are beginning to be introduced to synthesize inorganic materials through robotic experimentation. For instance, a robot has been devised to experimentally search for new photocatalysts[28]. More recently, robotics have been integrated with sample preparation using synthesis recipes generated from natural-language models[27]. These studies are just a few examples of the emerging role of artificial intelligence (AI) in the search for new functional materials.

However exciting, such advances have been largely limited to crystalline materials with ordered structures, which can typically be described by small unit cells. For example, the crystal structure of rock salt (NaCl) is uniquely defined by a primitive unit cell containing only two atoms. By contrast, glasses and other amorphous solids – which do not have translational symmetry and therefore no simple unit cells – are highly challenging to characterize, both for computational and experimental research[29–31], and these challenges have built up barriers over the years. For example, the DFT-based materials modelling approaches mentioned earlier are restricted to small simulation cells (typically a few hundred atoms) and short timescales (typically a few hundred picoseconds), even on fast supercomputers, because of the high computational cost and unfavourable system-size scaling behaviour of DFT. Consequently, even the most expensive DFT simulations will inevitably create simplified models of the 'real thing'[32] – and so they cannot fully capture the nature of an amorphous material, for example, the presence of nanoscale heterogeneity[33].

And even if one were to successfully design amorphous structures in the computer, there are more challenges on the way to 'real-world' synthesis and manufacturing (Box 1); for example, amorphous solids are metastable with respect to the competing crystalline phases, and therefore one must avoid unwanted structural transitions (for example, crystallization into a more stable ordered structure), or changes to sample properties owing to fluctuations in experimental parameters. Because of these challenges, it is likely that many amorphous materials with promising functionality remain undiscovered so far.

In this Perspective, we argue that the computational design of amorphous materials is becoming an increasingly rewarding and timely research goal, enabled by new AI-driven and ML-driven approaches that are currently transforming materials research more widely. We discuss how applying AI to the unique challenges in the domain of amorphous solids can offer new opportunities for fundamental and applied materials research alike. Building on this discussion, we outline a road map for the computationally guided design of amorphous functional materials.

Amorphous materials for emerging technologies

We set the stage by briefly reviewing applications of amorphous materials in key technologies, justifying why these materials are now receiving increasing attention. We do so by using four example cases (Fig. 1).

The first example is given by lithium-ion and sodium-ion batteries (Fig. 1a), which are crucial for energy storage[34–40]. The challenges here involve designing suitable anode, cathode and solid-state electrolyte materials to reach higher energy densities, increase charging rates and improve safety. Although research so far has often focused on crystalline battery materials, their amorphous counterparts can have superior properties[41]: isotropic ionic conductivity, the absence of grain-boundary resistance, ample ion storage sites and chemical flexibility[42–44]. For example, amorphous lithium metal, as an anode material, outperforms crystalline lithium in terms of electrochemical reversibility[45]. Specifically, electrolytes with an amorphous-to-crystalline (a-Li:c-Li) content ratio exceeding 3:1 were shown to cycle more than 50 times and maintain a capacity retention of 59.2%, whereas the baseline electrode with comparable amorphous and crystalline content failed within 5 cycles[45]. Amorphous forms of elemental carbon, including 'hard' (non-graphitizing) and 'soft' (graphitizing) ones, have been found suitable as Na-ion battery anodes based on offering either high reversible capacities[46,47] or conductivity for Na ions[48]. Amorphous solid-state electrolytes, such as a-Li_2S–P_2S_5 (ref. 49), a-$NaTaCl_6$ (ref. 50) and a-Na–Y–Zr–Cl compounds[51], exhibit superior ionic conductivity and electrochemical stability in solid-state Li-ion and Na-ion batteries.

The second example are phase-change materials (PCMs) (Fig. 1b), which are used in digital data storage and computing. Phase-change devices make use of a property contrast between a crystalline phase ('one bit') and an amorphous phase ('zero bit') to encode digital information[4]. The associated phase transitions need to occur rapidly and reversibly, while retaining the long-term stability of the amorphous zero bits. Ternary Ge–Sb–Te alloys are commonly used for this purpose. In fact, by adjusting the stoichiometric composition, frequently along the GeTe–Sb_2Te_3 line of the ternary phase diagram[52], various PCMs with distinct crystallization rates and temperatures have been found: $Ge_8Sb_2Te_{11}$ for optical discs[53], $Ge_1Sb_2Te_4$ for non-volatile data storage more generally[54] and $Ge_2Sb_2Te_5$ for neuromorphic (brain-inspired) computing devices[55], among others. Alloying with guest elements is another strategy for tailoring the properties of PCMs. For example, doping the parent compound Sb_2Te_3 with scandium[56] or yttrium[57] can speed up crystallization by enabling fast nucleation, whereas the crystallization temperature and resistivity of Sb_2Te_3 films can be enhanced by doping with silicon[58].

Box 1 | Challenges and opportunities for amorphous materials

What makes amorphous materials so interesting? Compared with their crystalline counterparts, they pose unique challenges.

No equilibrium structure
Amorphous solids are fundamentally out of thermodynamic equilibrium. Thus, they are prone to (re-)crystallization, particularly at high temperatures. In addition, the metastability of amorphous materials makes property measurements challenging: the experiment may affect the sample, for example, inducing crystallization if the material is heated during the measurement (for example, in microscale thermal conductivity measurements using laser-based techniques).

No unique synthesis recipe
Achieving precise control over structure and properties of amorphous materials remains a challenge: small variations in synthesis conditions can lead to changes in the final product. For example, noble-metal amorphous or nanostructured materials are promising catalysts for chemical reactions such as hydrogenation, oxidation and the oxygen evolution reaction[195,196]. However, traditional synthesis methods mostly yield crystalline, rather than amorphous, forms of these materials[197].

No direct structure determination (in most cases)
It is very challenging to determine the 3D atomic packing of amorphous materials owing to their lack of long-range order[29,30]. Advanced techniques, such as in situ NMR[198,199], can only characterize structures in a statistic sense, and simulations can only approximate the real structure. This lack of unique structural information challenges the accurate computational prediction of mechanical, thermal and electrical properties.

However, there are also unique opportunities.

Enhanced material performance
Amorphous materials can exhibit superior properties compared with their crystalline counterparts. For example, they lack grain boundaries, leading to enhanced ionic conductivity in solid-state electrolytes[200,201]. Amorphous materials can be melded into any form, which is exploited in bulk metallic glasses for mechanical applications, enabling precise shapes and high durability[84].

Higher compositional flexibility
Amorphous materials offer greater compositional flexibility compared with their crystalline counterparts. For example, although SiO does not exist in a stable crystalline phase, one can create nanostructured amorphous forms of SiO (refs. 33,202,203).

Tailored functional properties
The disordered nature of amorphous materials, once 'brought under control' synthetically, can allow for a wide range of tuneable properties, making it possible to design materials with specific functionalities for applications such as flexible electronics[204], high-strength coatings[205] and biocompatible implants[206].

Novel manufacturing techniques
Emerging synthesis and processing methods, such as ultrafast quenching[207], additive manufacturing[208] and ligand-exchange-induced amorphization[209], open up further possibilities for creating complex amorphous structures and components. Although the synthesis of crystalline materials has been perfected over many decades, it is likely that further, advanced routes for making amorphous materials are yet to be developed.

Notably, many of the challenges associated with amorphous materials are parallel to those encountered in the study of nanoparticles: no periodic boundary conditions, unique synthesis recipe or direct structure determination[210]. Consequently, new strategies developed for computational materials design in amorphous systems may offer analogous solutions for nanoparticles.

The third example in this section is given by photoelectrocatalysis (Fig. 1c), a technique to capture and convert energy from sunlight[59–61]. Here, the challenge is to design high-performing yet durable catalysts for a range of fundamental chemical transformations, including the hydrogen evolution reaction (HER) and oxygen evolution reaction (OER) that take place in water splitting. By leveraging localized and band tail states, amorphous materials can facilitate electron transport through hopping conductivity rather than band conduction in photoelectrocatalysis, resulting in improved conductivity[62]. In addition, compared with crystalline materials, amorphous catalysts typically have a larger electrochemical surface area, abundant catalytically active defect sites and high structural flexibility, leading to enhanced photocurrent, lowered overpotential and reduced carrier recombination[63]. Accordingly, multiple studies showed improvements in photoelectrocatalytic water splitting when using amorphous materials as catalysts. For example, a-FeOOH has shown high activity, broad pH adaptability and the ability to form uniform protective layers — enhancing the performance and durability of water-splitting systems[64]. Moreover, a-NiFeMo distinguishes itself from its crystalline counterparts by swiftly reforming its surface into a metal oxy(hydroxide) layer containing many oxygen vacancies during the OER, leading to higher catalytic performance at reduced overpotentials compared with crystalline materials[65]. Many other amorphous catalysts continue to be discovered and used, such as a-MoS_2 (refs. 66,67) and amorphous layered double hydroxides[68,69].

Our last example relates to nonlinear optical materials based on vapour-deposited molecular glasses (Fig. 1d) — a class of amorphous films frequently used in organic optoelectronic devices[70,71] owing to their capacity to exhibit spontaneous orientation polarization[72] arising from the collective orientation of molecules. A key research challenge here is to actively control the molecular orientation and the resultant polarization to optimize device performance. In a notable work in this area, donor–acceptor compounds based on the

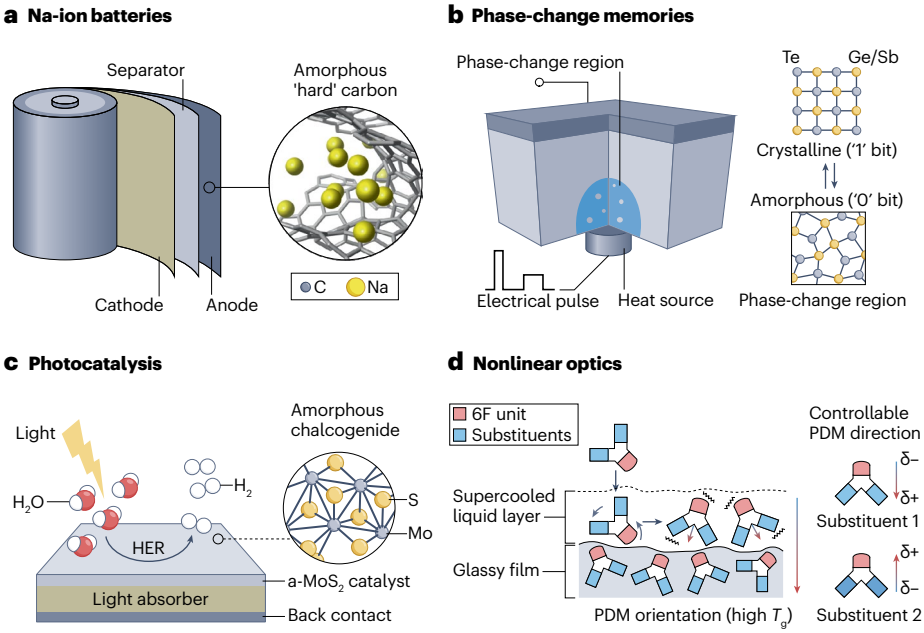

Fig. 1 | Amorphous materials for emerging technologies. a, Na-ion batteries. Computer simulations show that structural defects in amorphous carbon can provide sites for alkali-metal-ion absorption and clustering[191]. The structure in the inset is based on data from an earlier study[192] (only parts of the carbon network are shown). **b**, Phase-change memories. Adding a dopant element, in this case, scandium, improves the nucleation behaviour of Ge/Sb–Te materials[56] — providing an example of how not just the structure but also the dynamics of amorphous materials are amenable to chemical 'design'. **c**, Photocatalysis. Amorphous MoS_2, with its intrinsic and stable short Mo–Mo bonds, offers higher electrocatalytic activity and stability than crystalline phases[67]. A structural snapshot of a cluster model, used to represent the amorphous material in ref. 67, is shown in the inset. **d**, Nonlinear optics. The spontaneous orientation polarization of amorphous materials was leveraged to achieve films with a tuneable permanent dipole moment (PDM) by pairing the hexafluoropropane (6F) group with various substituents, where a supercooled liquid layer forms on the film surface during deposition, enabling molecular orientation changes to minimize surface free energy[73]. HER, hydrogen evolution reaction. Panel **a** schematic on the left adapted from ref. 36, Springer Nature Limited. Panel **b** adapted from ref. 97, CC BY 4.0. Panel **d** adapted from ref. 73, Springer Nature Limited.

hexafluoropropane (6F) group, paired with a set of substituents, were used to create amorphous films with spontaneous orientation polarization[73]. The films exhibited tuneable polarization properties controlled by the specific donor–acceptor pairing and deposition conditions, demonstrating a strong dependence on molecular orientation. The substrate temperature was found to influence molecular orientation, with lower temperatures favouring dipole alignment, whereas higher temperatures reduced the spontaneous orientation polarization effect, revealing the balance between molecular kinetics and surface energy in optimizing film properties. Notably, these films retained an overall amorphous configuration, as shown by X-ray diffraction. This work on spontaneously polarized organic glassy films, which can find applications in designing nonlinear optical components, optoelectronic devices such as organic light-emitting diodes and energy-harvesting technologies, shows the growing importance of organic amorphous materials.

Beyond the four selected cases in Fig. 1, amorphous materials are widely used in many other fields — such as solar cells[62], flexible electronics[74], thermoelectric devices[75], radiation detectors[76], thermal barrier coatings[77] and biomedical technologies[78]. For example, amorphous solids can show ultralow lattice thermal conductivity and superior mechanical properties (such as plastic deformation and bending) compared with their crystalline counterparts, making them promising candidates for self-powered wearable devices. Amorphous $Ag_2Te_{0.6}S_{0.4}$ has a peak thermoelectric figure of merit of about 0.7, along with a high tensile strain of ~12.5% (ref. 79) far exceeding the 1.5% limit typical of conventional inorganic thermoelectric fibres[80]. Amorphous silica nanoparticles have been widely used in drug delivery for cancer treatments and other medical therapies: their adjustable pore size and surface chemistry allow them to carry a broad range of drug types, including small-molecule therapeutics, nucleic acids and protein-based cargoes[81]. Finally, the recent synthesis of monolayer amorphous carbon ('amorphous graphene')[82], which exhibits high strength and tuneable electrical conductivity[83], has opened up new possibilities for applications in ultrathin flexible electronics. Note that this Perspective focuses on the functional properties of amorphous materials rather than on purely structurally based properties such as high hardness in bulk metallic glasses, which also have applications ranging from tools to medical devices[84].

The variety of examples discussed in this section shows that the structural diversity of amorphous materials — ranging from a seemingly simple elemental system (amorphous carbon) (Fig. 1a) all the way to complex molecular glasses (Fig. 1d) — can directly underpin a range of important technological applications. But what exactly does the structure of these materials look like?

Realistic models of amorphous structures

We need to create realistic structural models of amorphous solids before we can computationally predict (and subsequently optimize) their properties. Compared with crystalline phases with well-defined

unit cells, we will never be able to describe an amorphous structure exactly, so instead we are looking for the model that best approximates it within a given length scale and within our computational resource budget.

The most direct way to simulate atomic structures is by molecular dynamics (MD): computing the forces acting on the atoms in a structure and integrating Newton's equations of motion to describe their movement over time. MD simulations are now a mainstay of materials modelling, in general, and of modelling amorphous materials, in particular. There are two main types of approaches in this field. On the one hand, the community has long used melt–quench-type MD simulations: the rapid quenching of a simulated liquid leading to a 'frozen' amorphous configuration (Fig. 2a, top). Small-scale melt–quench simulations driven by DFT have been used early on to describe amorphous elemental systems[85,86] and PCMs[87,88] and are now very common, to the extent that they can be carried out in a largely automated fashion[89]. On the other hand, it is desirable — and at some point, necessary — to describe amorphous materials in a more realistic way: moving from small-scale melt–quench simulations (typically with a few hundred atoms at a time) to explicit, large-scale simulations of the physico-chemical mechanisms by which a given structure forms, requiring thousands of atoms or more.

In recent years, ML-based interatomic potentials, or force fields, have been used to address this challenge[90–92]: ML potentials are trained on DFT data and reach similar accuracy, while being able to describe much larger and therefore more realistic structural models — such as the explicit simulation of a reaction during material preparation (Fig. 2b, top). For amorphous solids, this means that the length-scale barrier has now essentially been broken, and quantum-mechanically accurate simulations of systems spanning tens of nanometres are almost routinely possible if one has high-performance computing systems available. In the context of amorphous materials, we can therefore now study fundamental problems such as structural changes in disordered matter under pressure[93–96], as well as application-related questions: an example is the recently reported 'device-scale' modelling of PCMs that are used in digital memories[97].

The bottom panel of Fig. 2a shows amorphous carbon as an example of melt-quenched structures: this figure emphasizes how the coordination environment of the atoms in the quenched structures is strongly influenced by the mass density of the sample. The higher the density, the more likely one is to find tetrahedral, diamond-like ('sp^3') motifs, but in almost all cases there is a mixture of those with graphite-like ('sp^2') environments[98]. Besides the density, the quench rates and system sizes also strongly affect the short-range and medium-range order of structural models obtained from melt–quench MD[99,100]. For example, quenching silicon at a rate of 10^{11} K s^{-1} gives a-Si structural models that compare well with experimental data[101]. Furthermore, one needs a

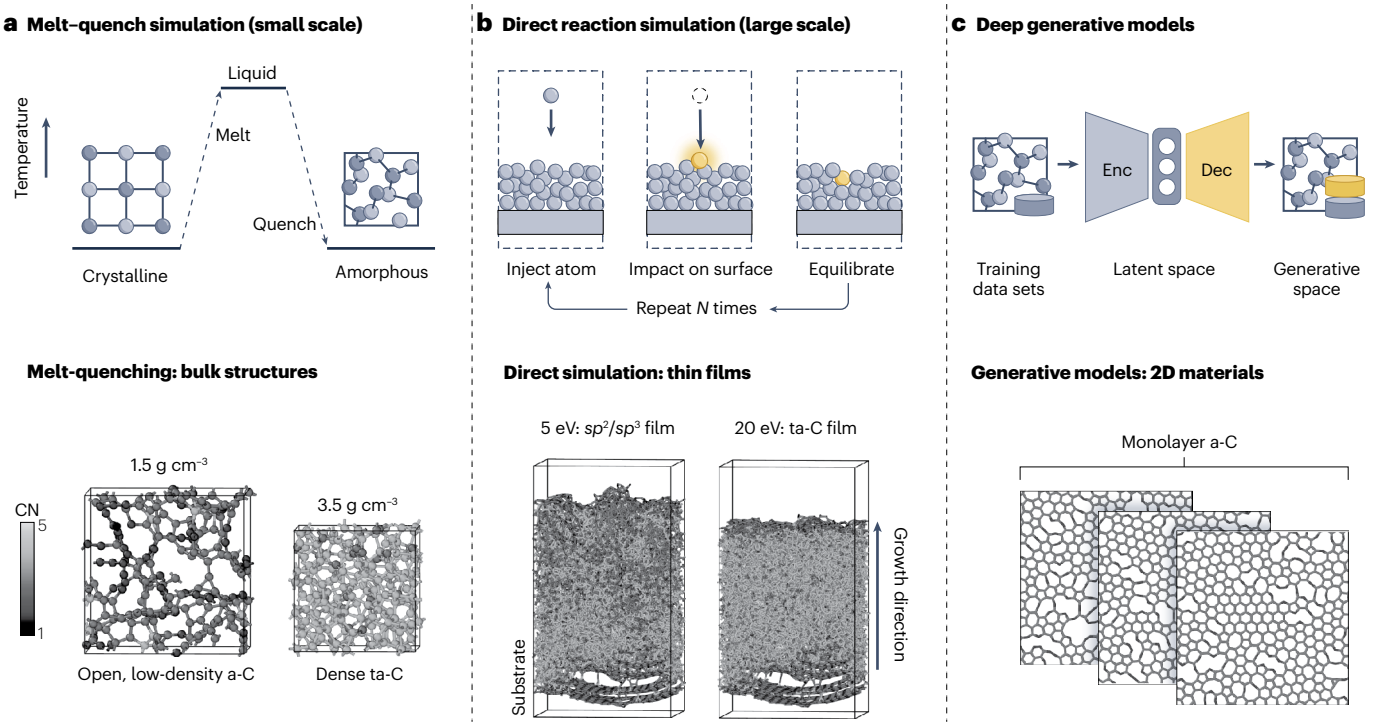

Fig. 2 | Simulating structures of amorphous materials. a, Melt–quench simulations for creating small-scale structural models. The schematic (top) illustrates the temperature profile of a typical simulation leading from an ordered crystalline structure to the liquid and onwards to a disordered amorphous configuration. The bottom panel shows two structural models of amorphous carbon at different densities obtained by machine-learning-driven melt–quench simulations, drawn with data from ref. 98. **b**, Realistic simulations of reactions for creating large-scale structural models of amorphous materials (top). The schematic illustrates the protocol for simulating the growth of amorphous carbon films by ion deposition. The bottom panel shows two carbon films created in machine-learning-driven deposition simulations, having been grown at different impact energies, drawn with data from ref. 105. **c**, Deep generative models (top) which compress training data using an encoder network (Enc) and decode the learned representation in latent space to generate a new structure (Dec). Three snapshots of an 'amorphous graphene' structural model are shown (bottom), drawn with data from ref. 113. The three subfigures at the bottom share the same colour bar range. a-C, amorphous carbon; CN, coordination number; ta-C, tetrahedral amorphous carbon. Panel **b**, top, adapted with permission from ref. 105, APS.

sufficiently large system, or many simulations in parallel, to collect adequate statistical data for properties such as defects in a finite-sized simulation[102]. Although melt–quench simulations have long been carried out with DFT for small-scale models, as discussed, ML potentials can be particularly helpful to reach slower quenching rates and larger sample sizes. In some cases, the mechanical[98] or thermal properties[103] of amorphous solids can already be reasonably reproduced using melt-quenched structures.

The bottom panel of Fig. 2b shows a result obtained with ML-driven MD for an 'explicit' reaction simulation: the growth of a-C thin films, as an example of the synthesis routes for amorphous materials based on deposition from atomic or molecular precursors. In this example, an atom-by-atom description of the deposition of tetrahedral amorphous carbon (ta-C), as well as lower-density films, achieved close agreement with the sp^3 count observed experimentally, thus enabling a microscopic understanding of the growth mechanisms[104,105]. This study allowed for correlating the energy of impacting ions with the densities and structural features of the resulting films: at low impact energy, low-density, sp^2-rich films were formed, and progressively mixed sp^2/sp^3 structures occurred; higher impact energies favoured the formation of dense, highly sp^3-rich ta-C films (20 eV and above)[104,105]. Beyond elemental carbon, many more amorphous inorganic materials can be grown by the chemical vapour deposition (CVD) of complex molecular precursors[106–109], and mechanistic insights could be gained from advanced simulations, in the same way that organic chemists now routinely describe molecular reactions with computer simulations. We expect much progress in this area in the years ahead.

ML-driven atomistic simulations are making impressive progress, but even the fastest ML potentials will only be able to visit a small fraction of all possible configurations for a given chemical system. This challenge is particularly pronounced for the many possible (metastable) local structures that atoms in amorphous materials can adopt and for complicated synthesis pathways, for example, in solution-based reactions (that will invariably be more complex than the example shown in Fig. 2b). Hence, beyond explicit MD simulations driven by ML potentials, there is a growing need for entirely new approaches to generating and screening amorphous materials with desired properties. Ultimately, generative models (Fig. 2c, top), a class of deep-learning ML methods, could help: by learning the probability distribution of structures, these models can sample more efficiently or even 'invent' new candidate molecules or materials, which may then be tested in atomistic simulations and subsequently in experiments. Examples of such generative models are currently being established for organic chemistry, having been used to search for new potential photoactive molecules and to suggest synthesis targets[110–112]. In the area of amorphous materials, a few studies to date have demonstrated the promise of generative models: for instance, they enabled the rapid generation of monolayer (2D) amorphous carbon structures with arbitrary model system size[113] (Fig. 2c, bottom). The development of similar generative methods for the even more complex case of 3D extended amorphous systems, however, is still at a very early stage[114,115].

There are two other important aspects that we cannot cover here in detail. One is the use of an activation–relaxation technique, which is well established in the field of a-Si and related materials[116,117]; this is discussed in a complementary review by some of the present authors[118]. The other is the use of experimental information in structure characterization: from established (hybrid) reverse Monte-Carlo techniques[119,120] to the use of deep-learning methods to automate the analysis of transmission electron microscopy images of monolayer amorphous carbon[121] or the inclusion of machine-learned X-ray spectroscopy fingerprints to inform atomistic modelling[122].

We close with a brief word of caution. The accuracy of structural models fundamentally depends on how well the model captures the short-range and medium-range atomic order, as these are critical in determining material properties. This structural accuracy must be validated through comparison with experimental data — obtained, for example, from scattering, spectroscopy or imaging measurements. Key metrics include the peak positions, shapes and intensities of the structure factors measured in scattering experiments, and the real-space pair distribution function that can be calculated from those data. By comparing experiment and simulation, one can gain confidence that the model captures essential features of the amorphous structure. However, this validation process remains fundamentally dependent on high-quality experimental data and on accurate simulations of scattering, spectroscopy and imaging data. In particular, the simulations must closely mirror the complexities of the experimental techniques[123,124].

Connecting structure and properties

Once the atomistic structure of an amorphous material is accurately known — and only then — it can be linked to structural and functional properties: the mechanical hardness, the bistability or multistability, the response of material to external stimuli or the electronic or thermal conductivity. Having discussed the creation of accurate structural models (Fig. 2), we now review computational approaches that take these structures as input and yield physical properties as output (Fig. 3a). These properties in turn allow us to judge whether a given amorphous material is useful for practical applications.

The material properties discussed in this Perspective are typically those that arise on the atomic scale — for example, mechanical hardness is a direct consequence of the strength of the bonding between atoms. To predict some of the more complex properties, one needs a full description of the potential-energy surface, which can now be achieved efficiently with a combination of DFT and fast ML potentials. For example, MD simulations can describe the thermal motion of atoms and therefore the resulting thermal conductivity, and DFT-trained ML potentials give access to large enough simulation cells to predict the thermal behaviour of nanostructured and amorphous materials[125–127]. In this context, it was shown that changing the composition of co-sputtered samples, and thereby the local atomic environments in the resulting amorphous material, can be used to easily tune the thermal conductivity[126]. Such predictions are typically tested on known (and experimentally well-characterized) materials first and can then be applied to new, previously unexplored reaction conditions. In other cases, property prediction may not require the use of a full ML potential model, but can be reduced to a simpler regression task in which the structure or even 'just' the composition of a material is mapped directly onto the relevant physical property — this is a common theme for crystalline materials[128,129], but will likely be of limited use on its own when it comes to amorphous materials (different samples of the same composition may have very different properties).

In the schematic of Fig. 3a, we highlight in red the important role of atomic structure particularly for the amorphous state. This is because the structure determination from composition is a substantially more challenging task in amorphous systems compared with crystalline ones (Box 1). The complexity arises from the vast configurational space and the presence of multiple potentially relevant metastable states: for example, amorphous PCMs (digital zero bits)

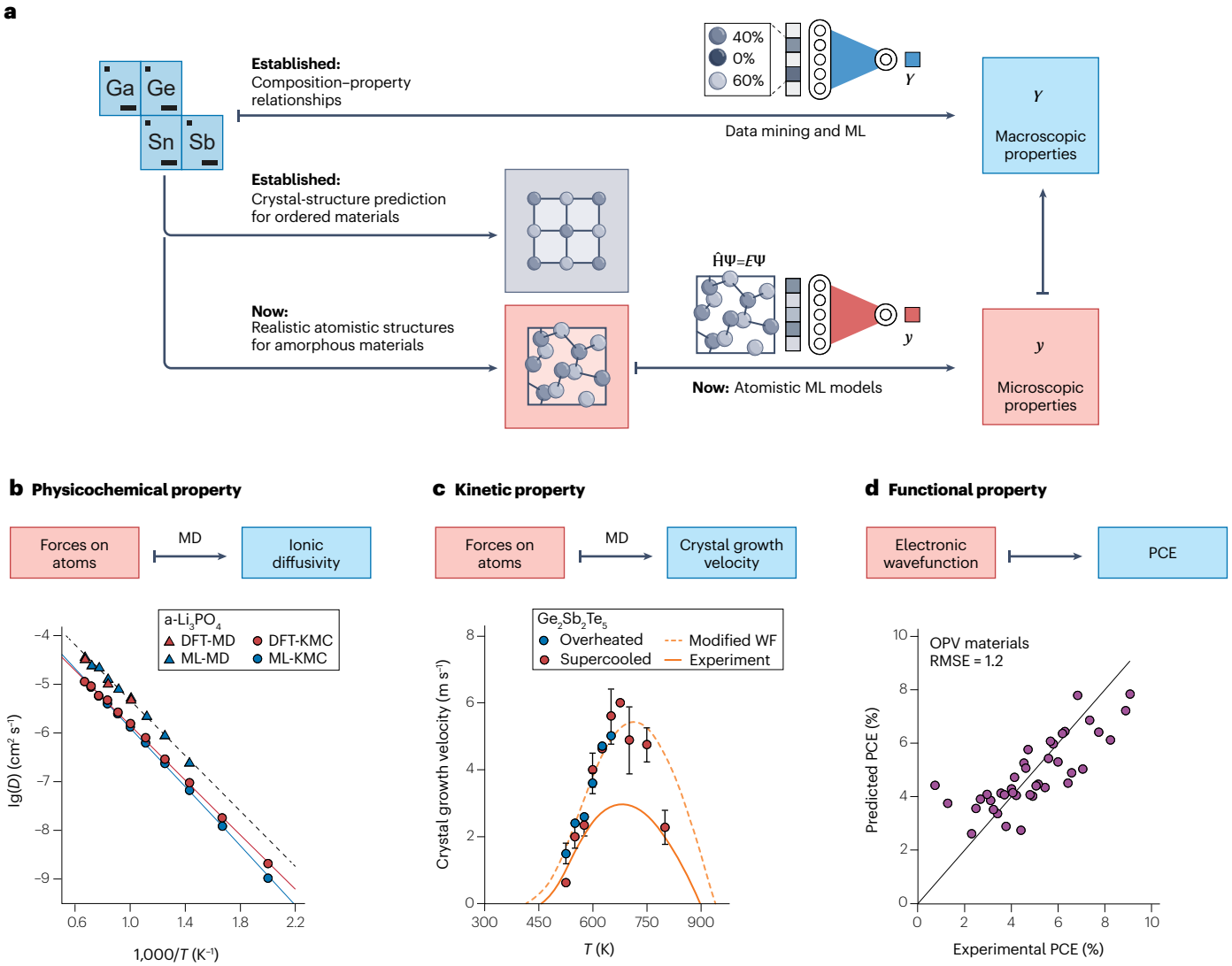

Fig. 3 | Predicting properties of amorphous materials. a, Schematics of how material properties can be predicted using computational techniques. Prediction of macroscopic properties, denoted *Y*, based on the chemical composition. Such tasks are well established in current materials research and can typically be carried out with the help of data-mining approaches and machine-learning (ML) models (top). Prediction of microscopic properties, denoted *y*, that depend on the local structure of an individual atom in the material (bottom). The structure prediction of crystalline materials (grey) is a well-established task. Beyond crystalline phases, the creation of realistic structural models of amorphous materials (red) is now coming within reach. Once those structures are known, atomistic ML models can be trained on quantum-mechanical data to predict microscopic properties — those, in turn, give rise to the target macroscopic property. **b**, Li-ion diffusion coefficients, *D*, in amorphous Li_3PO_4 predicted by molecular dynamics (MD) and kinetic Monte-Carlo (KMC) simulations driven by a neural-network potential[132]. The MD and KMC simulations are qualitatively consistent, whereas the quantitative difference arises from the use of a uniform jump frequency for all transitions in the KMC simulation. The solid and dashed lines represent linear fits based on the Arrhenius law, used to determine the effective activation energy for diffusion. **c**, Crystal growth velocities of overheated amorphous and supercooled liquid $Ge_2Sb_2Te_5$ phases as a function of temperature[136]. The dashed line represents the fit using a modified Wilson–Frenkel (WF) formula, which is effective to describe the crystal growth velocity in the supercooled liquid[136,138]. The available experimental data (solid line) come from differential scanning calorimetry[137]. **d**, Comparison between experimental power conversion efficiencies (PCEs) of organic photovoltaic (OPV) materials and predicted values by combining a graph neural network and a LightGBM model[110,193]. LightGBM is a highly efficient gradient boosting framework widely used for regression and classification tasks on large data sets. DFT, density-functional theory; RMSE, root mean squared error.

age over time, changing their resistance value[130], and CVD involves a series of complex physical and chemical surface processes, including diffusion, adsorption of molecules and subsequent reactions[109]. As a result, determining the correct atomic arrangements is a key step in linking composition to property, and it is even more difficult than property prediction itself.

To illustrate what is currently possible in this area, we show in Fig. 3b–d three cases in which properties of amorphous materials have

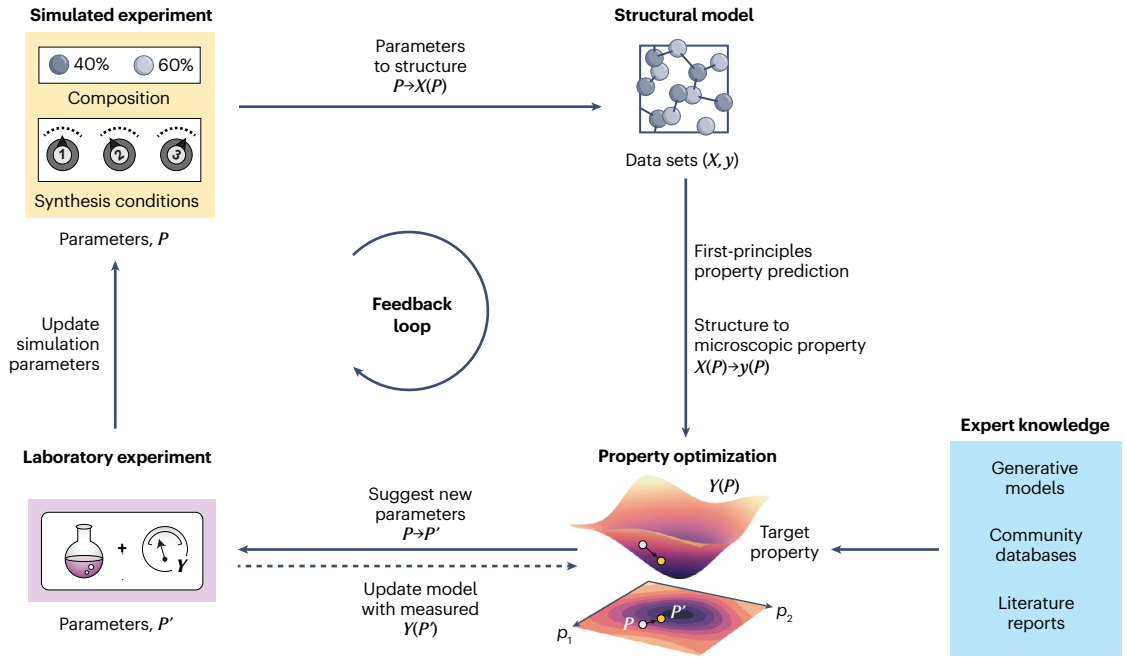

Fig. 4 | A closed-loop perspective for amorphous materials design. On the basis of a simulated experiment with given parameters, a structural model is obtained, providing the mapping from parameters to structure (Fig. 2). The next mapping, from structure to property, is achieved by property prediction models (Fig. 3). Together, these approaches allow to predict a target property as a function of experimental parameters. We denote the structural model as a set of coordinates $X = \{\mathbf{x}_1, \mathbf{x}_2, ...\}$; similarly, we denote the set of all relevant synthesis parameters as $P = \{p_1, p_2, ...\}$[194]. Finally, we call the atomic property of interest y and the macroscopic property of interest Y. In this notation, property prediction therefore means learning the function $Y(P)$ for complex simulated structures. The next step involves optimizing the macroscopic property, a process that can furthermore be informed by using expert knowledge — encoded, for example, in previous literature reports or community databases. The computational optimization of $Y(P)$ (ref. 175) leads to a suggestion of new and improved parameters, P', which can be tested in laboratory experiments and the simulation repeated — thereby closing the feedback loop. The experimental observations could also provide an additional source of information for the model, which is indicated by a dashed line.

been successfully predicted from first principles (by 'first principles', we mean the use of quantum mechanics or of quantum-mechanically accurate ML models, or a combination of both). The first case is given by battery materials, specifically a-Li_3PO_4 solid-state electrolytes, in which the diffusion coefficients of Li-ions were predicted using MD driven by a Behler–Parrinello-type neural-network potential[131], in good agreement with DFT results[132] (Fig. 3b). Compositionally flexible ('universal') ML potentials, such as M3GNet[133] and CHGNet[134], are capable of accurately predicting the Li-ion diffusion coefficients of more than 5,000 amorphous materials[135]. The second example is given by the crystallization kinetics of the PCM $Ge_2Sb_2Te_5$ (ref. 136) (Fig. 3c). The crystal growth velocities in overheated amorphous and supercooled liquid phases were modelled with ML-driven MD simulations involving more than 10,000 atoms for more than 100 ns, qualitatively reproducing experimental observations below 600 K (ref. 137). A modified form of the Wilson–Frenkel formula[136,138] was used to model the temperature-dependent crystal growth velocity in the supercooled liquid phase, offering a theoretical framework that complements the experimentally validated amorphous phase.

Turning again to molecular materials, the third case of property prediction concerns the power conversion efficiencies (PCEs) of organic photovoltaic materials[110] (Fig. 3d) in which crystalline and amorphous domains of donor and acceptor species are combined to form unique landscapes for charge percolation[139]. The direct simulation of PCEs is challenging owing to the need for an accurate understanding of electronic-structure properties (rather than 'just' the atomic structure) — namely, electronic energy levels, charge transport, exciton diffusion and recombination rates[140]. Additionally, factors such as the molecular orientation, active-layer morphology, the role of amorphous domains and donor–acceptor interface interactions add to the complexity. In this context, a purely data-driven ML surrogate model was proposed, which bypasses costly electronic-structure calculations and achieves predictions that align rather well with experimental results[110]. In addition, property-based ML (blue in Fig. 3a) is also beginning to be used to screen amorphous catalysts by accurately predicting electrochemical properties, such as site-averaged activation energies within chemical accuracy (below 0.75 kcal mol^{-1}) in a wide energy range of 40 kcal mol^{-1} (refs. 141–144).

Towards computational design

Building on the discussion so far, we now look forward and outline a conceptual framework for the 'self-guided' design of amorphous materials with target properties. We aim to complement existing work on materials design for crystalline solids[145,146] and to encourage future exploration in the growing area of amorphous materials. We envision that such a conceptual framework could, in due course, be developed into a fully automated discovery framework, capable of exploring the structural and chemical space beyond the much-better studied crystalline state — synthesizing amorphous materials, testing and optimizing their properties in a closed loop (Fig. 4). The key steps are as follows.

Training data

The development and curation of training data is a critical step in the construction of any ML model, atomistic or otherwise[147]. There have been substantial efforts in building computational databases for materials in general[148], and experimental property databases are beginning to be developed as well[149]. The data that will be required to train next-generation ML models in the specific domain of amorphous materials are likely to come from two main sources.

First, efficient ML-driven simulation techniques, ranging from simple melt-quenching (Fig. 2a) to realistic simulated reactions (Fig. 2b), can continue to be used to generate amorphous-phase structural models for which properties of interest may then be predicted. Looking back at the examples mentioned earlier, such simulations have already been used to create data sets of relevant amorphous materials, including a-C[98,105] and Ge–Sb–Te PCMs[100,150]. More extensive developments will be needed, not just for efficiently representing multicomponent systems (say, organic molecular materials) but also for obtaining the relevant quantum-mechanical data labels at scale.

Second, large pre-trained natural-language models can be used to data-mine existing literature for information on structures, syntheses or properties of materials[151], and we expect that they might become useful for amorphous solids as well. In brief, word embeddings such as Word2vec[152], GloVe[153], ELMo[154] or FastText[155] facilitate text mining by converting words into continuous vector spaces based on their context, capturing semantic similarities. For example, the Word2vec algorithm was used to generate unsupervised word embeddings from ~3.3 million scientific abstracts, enabling predictions of possible new thermoelectrics, photovoltaics and ferroelectrics[156]. This capability highlights the utility of unsupervised learning (without the need for human labelling) in extracting hidden patterns from large amounts of existing scientific literature. With the advent of sophisticated transformer models, such as Bidirectional Encoder Representations from Transformers (BERT)[157] and Generative Pre-trained Transformer (GPT)[158], text mining is evolving towards context-aware language understanding and generation. BioBERT, a domain-specific adaptation of BERT, was developed to enhance performance in biomedical text-mining tasks such as named entity recognition, relation extraction and question answering[159].

Although large language models (LLMs) are increasingly applied in the fields of crystalline materials and organic molecules[160–163], they have rarely been utilized for amorphous materials to date. A recent study classified experiments as successful or 'failed', and the formation of an amorphous phase was considered to be one of those failure categories[164]. Hence, one challenge is in the fact that only limited literature is available for amorphous materials. Moreover, training LLMs on biased, incomplete or inaccurate data sets can skew predictions[165] — and it has been noted that models trained on scientific literature may inherently focus on successful experiments[166]. This is particularly critical for amorphous materials, in which the current lack of well-structured data makes it difficult to train models in the first place. However, if in the future we can address these limitations through the generation of more comprehensive data sets covering the large amount of possible experimental outcomes, we expect AI-accelerated text mining to find increasing application in the field of amorphous materials.

Controlling synthesis conditions

Structures and properties of amorphous materials depend strongly on the synthesis conditions. Controlling synthesis is an even more critical challenge here than in most crystalline materials, and therefore existing approaches to materials design often do not yet integrate all available knowledge when planning materials syntheses. To address this problem, the design framework must reflect the experimental conditions, including the choice of method (physical or CVD, for example), the parameters, such as pressure and temperature, deposition rate or substrate material. Although current simulations do not yet fully capture the complexity of real-world experimental conditions, advances in different classes of ML techniques are bringing them progressively closer to an accurate representation. It is also important to consider the reproducibility of these conditions across different laboratories, to ensure the consistency of the materials produced. The latter point is important beyond amorphous materials: for example, a relevant study concerning crystalline metal–organic frameworks showed that the product obtained may differ substantially between different laboratories carrying out a given synthesis[167].

In our envisioned framework, the synthesis parameters, pertaining either to a simulation or to the actual experiment, are what ultimately controls the resulting atomic structures and properties. We therefore expect to feed information from an experiment back into the optimization cycle (Fig. 4). One potential approach in this context is to develop multimodal models that can process both simulation data and experimental results as input. Contextual adaptation could enable the model to adjust its interpretation of one input (for example, simulations) based on feedback from another input (for example, experiments) — similar to how LLMs can modify an image based on textual input. In our framework, this capability could allow the simulation parameters to adapt iteratively by incorporating experimental feedback, thereby refining the optimization process.

We also think that the scarcity of experimental observations could be offset by large amounts of accurate, 'synthetic' (simulation-based) data: predicting the target property for multiple simulated structures and using this information together with experimental properties to build data-intensive, deep-learning models.

Exploring and optimizing the functional space

In terms of automating the design of materials and molecules, Bayesian optimization (BO) is a popular approach — especially in cases in which data acquisition is expensive, as it predicts the most valuable next experiment to perform. BO uses a probabilistic model, typically a Gaussian process, to approximate an (unknown) objective function that relates material or molecular features to desired properties. This model is iteratively updated with data from each new experiment or simulation, as proposed by an acquisition function, refining the prediction of the shape of the objective function and thereby identifying the most promising regions to explore next. By balancing the exploration of unexplored areas with the exploitation of those that are already known, BO facilitates the discovery of optimal materials (and the experimental conditions that are required for this).

To date, BO has been successfully applied in various domains of materials or molecular design[168], including drug discovery[169], finding reaction parameters[170] and catalyst optimization[171], demonstrating its versatility and efficiency in navigating high-dimensional design spaces. Indeed, this versatility has extended to the design of amorphous materials as well. For example, BO associated with Gaussian process regression was used to identify the most relevant morphological features influencing the stability and performance of organic photovoltaics[172]. The results revealed that adding [70]PCBM can enhance the morphological order in acceptor phases, thereby improving device stability with environmentally friendly solvents.

Looking beyond BO, which faces challenges in tackling high-dimensional input spaces, other optimization algorithms established in ML research may provide more efficient solutions. As a popular heuristic search method, evolutionary algorithms, inspired by the process of natural evolution, prove to be particularly effective for multi-objective optimization, as they can explore multiple solutions in parallel and avoid getting trapped in local optima. Evolutionary algorithms were used for parameter optimization in the design of colloidal phases[173]. Deep-learning optimizers, such as stochastic gradient descent and RMSProp, provide another alternative to optimize parameters in a high-dimensional space by minimizing the error between predicted and desired material properties through the gradients. Additionally, deep reinforcement learning offers a powerful tool for complex optimization tasks through agent–environment interaction mechanisms, in which a 'decision-maker' takes a series of actions within a specific environment to maximize the total accumulated reward over time. Deep reinforcement learning was applied to the optimization of chemical reactions[174].

To explore the large space of potential compositions and synthesis conditions, 'inverse design' methods such as generative ML models could prove useful — for example, using an autoencoder (AE) architecture[175]. AEs map high-dimensional vectors into a low-dimensional latent space (encoder network) and then decompress the latent vector to original structures (decoder network). In this case, the input and output could combine the characteristics of structures and properties for a given material[175], treated separately or collected (concatenated) into a single vector. Through training, the model 'learns' to identify patterns in the input data and encodes them into a lower-dimensional representation that captures essential features. More sophisticated variations, such as variational AEs (VAEs), extend the approach by modelling the latent space using probability distributions rather than fixed points. For example, a VAE was used to reduce the dimensions of the search space in which BO was carried out, with an application to a lattice model representing a ferroelectric material[176]. Conditional VAEs incorporate property-specific inputs through dedicated neural networks, enabling the generation of structures conditioned on desired material properties. This approach enhances the ability of the model to generate meaningful, property-driven outputs, thereby enabling more targeted inverse design of materials. For nanoparticles, conditional VAEs have proven useful to solve the structure directly from scattering data[177,178]. We note in passing that other popular generative models, such as generative adversarial networks and diffusion models, have demonstrated potential as alternatives to VAEs[179].

Outlook

We have outlined our vision for how AI and ML techniques can unlock the computational design of amorphous materials. However, there are several remaining obstacles to realizing this vision in the near future.

A key challenge — as with many classes of ML models — is that training data are often scarce. The design of crystalline materials has long benefited from well-established databases such as the experimentally based Cambridge Structural Database[180] and the Inorganic Crystal Structure Database[181], computational platforms such as the Materials Project[148], and successful techniques for modelling disorder in crystals[182]. However, the development of comparable databases for amorphous materials (or their integration into existing ones) lags substantially behind, and existing data sets for amorphous materials are typically focused on specific classes of materials[183]. Two highly encouraging examples in the recent literature are the use of a computationally generated data set of quenched amorphous structural models, which were assessed for their suitability for use in batteries[184], and a recent report on a large database of MD-generated amorphous structures[135]. Without sufficient amounts of data, and fully-fledged databases, atomistic ML models for amorphous materials are likely to remain limited to specific material systems. In the area of language models, which we think hold promise in extracting information about amorphous materials from the scientific literature, there is still a major challenge in accurately identifying and structuring these data into a usable format for ML — even more so than for crystals.

A second challenge lies in the development of general-purpose ML potentials for atomistic simulations of amorphous materials. Although the architectures for fitting ML potentials are now highly sophisticated (reaching milli-electronvolt-per-atom accuracy, as accurate as the underlying DFT training data can be), it is still not trivial to train reliable potentials for amorphous materials — owing, for example, to the diversity of local atomic environments that need to be considered in training, compared with crystalline matter. However, recent work has shown that ML potentials can be (pre-)trained on very large data sets[133,134,185,186] and subsequently fine-tuned for a specific purpose[186–188], which holds promise for amorphous structures as well. Furthermore, active learning and automated protocols can help to generate relevant training data more quickly, requiring less 'domain knowledge' on the side of the user, accelerating the overall development process. An important long-term goal in this area will be the creation of a truly universal ML potential for modelling amorphous materials across the Periodic Table.

The final challenge, in our view, is to integrate the theoretical and computational design of amorphous materials with experimental synthesis and manufacturing. Similar to recent breakthroughs in the automated synthesis and characterization of crystalline materials[27,189] and thin films[190], one may envision a fully automated laboratory that can synthesize amorphous materials with target properties. Compared with crystalline materials, however, amorphous materials typically require more specialized synthesis methods. Ensuring the reproducibility of these syntheses across laboratories will be important, and reliable, automated characterization approaches are likely to be essential for the preparation of amorphous materials at scale. Some of these characterization techniques (for properties, such as the electronic conductivity) can be borrowed from research on crystalline materials, whereas others (for the atomistic structure) will be different, often much more challenging (Box 1) and will therefore need to go beyond those already used for crystals. Once these challenges have been overcome, the genuine design of amorphous materials for batteries, solar cells, catalysts and many other applications would come within reach, facilitating unprecedented innovation in materials research.

Published online: 16 December 2024

References

1. Nayak, P. K., Mahesh, S., Snaith, H. J. & Cahen, D. Photovoltaic solar cell technologies: analysing the state of the art. *Nat. Rev. Mater.* **4**, 269–285 (2019).
2. Kuzum, D., Jeyasingh, R. G. D., Lee, B. & Wong, H.-S. P. Nanoelectronic programmable synapses based on phase change materials for brain-inspired computing. *Nano Lett.* **12**, 2179–2186 (2012).
3. van de Burgt, Y., Melianas, A., Keene, S. T., Malliaras, G. & Salleo, A. Organic electronics for neuromorphic computing. *Nat. Electron.* **1**, 386–397 (2018).
4. Zhang, W., Mazzarello, R., Wuttig, M. & Ma, E. Designing crystallization in phase-change materials for universal memory and neuro-inspired computing. *Nat. Rev. Mater.* **4**, 150–168 (2019).
5. Mannsfeld, S. C. B. et al. Highly sensitive flexible pressure sensors with microstructured rubber dielectric layers. *Nat. Mater.* **9**, 859–864 (2010).

6. Laurila, T., Sainio, S. & Caro, M. A. Hybrid carbon based nanomaterials for electrochemical detection of biomolecules. *Prog. Mater. Sci.* **88**, 499–594 (2017).
7. Kaspar, C., Ravoo, B. J., van der Wiel, W. G., Wegner, S. V. & Pernice, W. H. P. The rise of intelligent matter. *Nature* **594**, 345–355 (2021).
8. Keen, D. A. & Goodwin, A. L. The crystallography of correlated disorder. *Nature* **521**, 303–309 (2015).
9. Simonov, A. & Goodwin, A. L. Designing disorder into crystalline materials. *Nat. Rev. Chem.* **4**, 657–673 (2020).
10. Elliott, S. R. Medium-range structural order in covalent amorphous solids. *Nature* **354**, 445–452 (1991).
11. Wright, A. C. The great crystallite versus random network controversy: a personal perspective. *Int. J. Appl. Glass Sci.* **5**, 31–56 (2014).
12. Tanaka, H., Tong, H., Shi, R. & Russo, J. Revealing key structural features hidden in liquids and glasses. *Nat. Rev. Phys.* **1**, 333–348 (2019).
13. Savoie, B. M. et al. Mesoscale molecular network formation in amorphous organic materials. *Proc. Natl Acad. Sci. USA* **111**, 10055–10060 (2014).
14. Kim, S., Agarwala, A. & Chowdhury, D. Fractionalization and topology in amorphous electronic solids. *Phys. Rev. Lett.* **130**, 026202 (2023).
15. Nomura, K. et al. Room-temperature fabrication of transparent flexible thin-film transistors using amorphous oxide semiconductors. *Nature* **432**, 488–492 (2004).
16. Smith, R. D. L. et al. Photochemical route for accessing amorphous metal oxide materials for water oxidation catalysis. *Science* **340**, 60–63 (2013).
17. Han, F. et al. High electronic conductivity as the origin of lithium dendrite formation within solid electrolytes. *Nat. Energy* **4**, 187–196 (2019).
18. Hong, S. et al. Ultralow-dielectric-constant amorphous boron nitride. *Nature* **582**, 511–514 (2020).
19. Heo, J. et al. Amorphous iron fluorosulfate as a high-capacity cathode utilizing combined intercalation and conversion reactions with unexpectedly high reversibility. *Nat. Energy* **8**, 30–39 (2022).
20. Hautier, G., Jain, A. & Ong, S. P. From the computer to the laboratory: materials discovery and design using first-principles calculations. *J. Mater. Sci.* **47**, 7317–7340 (2012).
21. Saal, J. E., Kirklin, S., Aykol, M., Meredig, B. & Wolverton, C. Materials design and discovery with high-throughput density functional theory: the Open Quantum Materials Database (OQMD). *JOM* **65**, 1501–1509 (2013).
22. Butler, T. et al. Computational materials design of crystalline solids. *Chem. Soc. Rev.* **45**, 6138–6146 (2016).
23. Jain, A., Shin, Y. & Persson, K. A. Computational predictions of energy materials using density functional theory. *Nat. Rev. Mater.* **1**, 15004 (2016).
24. Gorai, P., Stevanović, V. & Toberer, E. S. Computationally guided discovery of thermoelectric materials. *Nat. Rev. Mater.* **2**, 17053 (2017).
25. Therrien, F., Jones, E. B. & Stevanović, V. Metastable materials discovery in the age of large-scale computation. *Appl. Phys. Rev.* **8**, 031310 (2021).
26. Merchant, A. et al. Scaling deep learning for materials discovery. *Nature* **624**, 80–85 (2023).
27. Szymanski, N. J. et al. An autonomous laboratory for the accelerated synthesis of novel materials. *Nature* **624**, 86–91 (2023).
28. Burger, B. et al. A mobile robotic chemist. *Nature* **583**, 237–241 (2020).
29. Miao, J., Ercius, P. & Billinge, S. J. L. Atomic electron tomography: 3D structures without crystals. *Science* **353**, aaf2157 (2016).
30. Yang, Y. et al. Determining the three-dimensional atomic structure of an amorphous solid. *Nature* **592**, 60–64 (2021).
31. Yuan, Y. et al. Three-dimensional atomic packing in amorphous solids with liquid-like structure. *Nat. Mater.* **21**, 95–102 (2022).
32. Chang, C., Deringer, V. L., Katti, K. S., Van Speybroeck, V. & Wolverton, C. M. Simulations in the era of exascale computing. *Nat. Rev. Mater.* **8**, 309–313 (2023).
33. Erhard, L. C., Rohrer, J., Albe, K. & Deringer, V. L. Modelling atomic and nanoscale structure in the silicon–oxygen system through active machine learning. *Nat. Commun.* **15**, 1927 (2024).
34. Yabuuchi, N., Kubota, K., Dahbi, M. & Komaba, S. Research development on sodium-ion batteries. *Chem. Rev.* **114**, 11636–11682 (2014).
35. Janek, J. & Zeier, W. G. A solid future for battery development. *Nat. Energy* **1**, 16141 (2016).
36. Choi, J. W. & Aurbach, D. Promise and reality of post-lithium-ion batteries with high energy densities. *Nat. Rev. Mater.* **1**, 16013 (2016).
37. Li, M., Lu, J., Chen, Z. & Amine, K. 30 years of lithium-ion batteries. *Adv. Mater.* **30**, 1800561 (2018).
38. Vaalma, C., Buchholz, D., Weil, M. & Passerini, S. A cost and resource analysis of sodium-ion batteries. *Nat. Rev. Mater.* **3**, 18013 (2018).
39. Nayak, P. K., Yang, L., Brehm, W. & Adelhelm, P. From lithium-ion to sodium-ion batteries: advantages, challenges, and surprises. *Angew. Chem. Int. Ed.* **57**, 102–120 (2018).
40. Grey, C. P. & Hall, D. S. Prospects for lithium-ion batteries and beyond — a 2030 vision. *Nat. Commun.* **11**, 6279 (2020).
41. Guo, T., Hu, P., Li, L., Wang, Z. & Guo, L. Amorphous materials emerging as prospective electrodes for electrochemical energy storage and conversion. *Chem* **9**, 1080–1093 (2023).
42. Jiang, Y. et al. Amorphous Fe_2O_3 as a high-capacity, high-rate and long-life anode material for lithium ion batteries. *Nano Energy* **4**, 23–30 (2014).
43. Lin, L., Xu, X., Chu, C., Majeed, M. K. & Yang, J. Mesoporous amorphous silicon: a simple synthesis of a high-rate and long-life anode material for lithium-ion batteries. *Angew. Chem. Int. Ed.* **128**, 14269–14272 (2016).
44. Ding, J., Ji, D., Yue, Y. & Smedskjaer, M. M. Amorphous materials for lithium-ion and post-lithium-ion batteries. *Small* **20**, 2304270 (2024).
45. Wang, X. et al. Glassy Li metal anode for high-performance rechargeable Li batteries. *Nat. Mater.* **19**, 1339–1345 (2020).
46. Stevens, D. A. & Dahn, J. R. High capacity anode materials for rechargeable sodium-ion batteries. *J. Electrochem. Soc.* **147**, 1271 (2000).
47. Stevens, D. A. & Dahn, J. R. The mechanisms of lithium and sodium insertion in carbon materials. *J. Electrochem. Soc.* **148**, A803 (2001).
48. Zhao, R., Sun, N. & Xu, B. Recent advances in heterostructured carbon materials as anodes for sodium-ion batteries. *Small Struct.* **2**, 2100132 (2021).
49. Kudu, Ö. U. et al. A review of structural properties and synthesis methods of solid electrolyte materials in the Li_2S–P_2S_5 binary system. *J. Power Sources* **407**, 31–43 (2018).
50. Hu, Y. et al. Superionic amorphous $NaTaCl_6$ halide electrolyte for highly reversible all-solid-state Na-ion batteries. *Matter* **7**, 1018–1034 (2024).
51. Ridley, P. et al. Amorphous and nanocrystalline halide solid electrolytes with enhanced sodium-ion conductivity. *Matter* **7**, 485–499 (2024).
52. Wuttig, M. & Yamada, N. Phase-change materials for rewriteable data storage. *Nat. Mater.* **6**, 824–832 (2007).
53. Akola, J. & Jones, R. O. Structure of amorphous $Ge_8Sb_2Te_{11}$: GeTe-Sb_2Te_3 alloys and optical storage. *Phys. Rev. B* **79**, 134118 (2009).
54. Kang, D.-H., Young Kim, N., Jeong, H. & Cheong, B. Understanding on the current-induced crystallization process and faster set write operation thereof in non-volatile phase change memory. *Appl. Phys. Lett.* **100**, 063508 (2012).
55. Ambrogio, S. et al. An analog-AI chip for energy-efficient speech recognition and transcription. *Nature* **620**, 768–775 (2023).
56. Rao, F. et al. Reducing the stochasticity of crystal nucleation to enable subnanosecond memory writing. *Science* **358**, 1423–1427 (2017).
57. Liu, B. et al. Y-doped Sb_2Te_3 phase-change materials: toward a universal memory. *ACS Appl. Mater. Interfaces* **12**, 20672–20679 (2020).
58. Zhang, Y. et al. Characteristics of Si-doped Sb_2Te_3 thin films for phase-change random access memory. *Appl. Surf. Sci.* **254**, 5602–5606 (2008).
59. Yang, J., Wang, D., Han, H. & Li, C. Roles of cocatalysts in photocatalysis and photoelectrocatalysis. *Acc. Chem. Res.* **46**, 1900–1909 (2013).
60. Zhang, L. et al. Photoelectrocatalytic arene C–H amination. *Nat. Catal.* **2**, 366–373 (2019).
61. Shan, B. et al. Binary molecular-semiconductor p–n junctions for photoelectrocatalytic CO_2 reduction. *Nat. Energy* **4**, 290–299 (2019).
62. Wang, B. M., Biesold, G., Zhang, M. & Lin, Z. Amorphous inorganic semiconductors for the development of solar cell, photoelectrocatalytic and photocatalytic applications. *Chem. Soc. Rev.* **50**, 6914–6949 (2021).
63. Anantharaj, S. & Noda, S. Amorphous catalysts and electrochemical water splitting: an untold story of harmony. *Small* **16**, 1905779 (2020).
64. Chemelewski, W. D., Lee, H.-C., Lin, J.-F., Bard, A. J. & Mullins, C. B. Amorphous FeOOH oxygen evolution reaction catalyst for photoelectrochemical water splitting. *J. Am. Chem. Soc.* **136**, 2843–2850 (2014).
65. Duan, Y. et al. Scaled-up synthesis of amorphous NiFeMo oxides and their rapid surface reconstruction for superior oxygen evolution catalysis. *Angew. Chem. Int. Ed.* **58**, 15772–15777 (2019).
66. Morales-Guio, C. G., Tilley, S. D., Vrubel, H., Grätzel, M. & Hu, X. Hydrogen evolution from a copper(I) oxide photocathode coated with an amorphous molybdenum sulphide catalyst. *Nat. Commun.* **5**, 3059 (2014).
67. Wu, L. et al. The origin of high activity of amorphous MoS_2 in the hydrogen evolution reaction. *ChemSusChem* **12**, 4383–4389 (2019).
68. Yu, L. et al. Amorphous NiFe layered double hydroxide nanosheets decorated on 3D nickel phosphide nanoarrays: a hierarchical core–shell electrocatalyst for efficient oxygen evolution. *J. Mater. Chem. A* **6**, 13619–13623 (2018).
69. Hu, Y. et al. Single Ru atoms stabilized by hybrid amorphous/crystalline FeCoNi layered double hydroxide for ultraefficient oxygen evolution. *Adv. Energy Mater.* **11**, 2002816 (2021).
70. Tang, C. W. & VanSlyke, S. A. Organic electroluminescent diodes. *Appl. Phys. Lett.* **51**, 913–915 (1987).
71. Noguchi, Y., Tanaka, Y., Ishii, H. & Brütting, W. Understanding spontaneous orientation polarization of amorphous organic semiconducting films and its application to devices. *Synth. Met.* **288**, 117101 (2022).
72. Ito, E. et al. Spontaneous buildup of giant surface potential by vacuum deposition of Alq_3 and its removal by visible light irradiation. *J. Appl. Phys.* **92**, 7306–7310 (2002).
73. Tanaka, M., Auffray, M., Nakanotani, H. & Adachi, C. Spontaneous formation of metastable orientation with well-organized permanent dipole moment in organic glassy films. *Nat. Mater.* **21**, 819–825 (2022).
74. Street, R. A. Thin-film transistors. *Adv. Mater.* **21**, 2007–2022 (2009).
75. Nolas, G. S. & Goldsmid, H. J. The figure of merit in amorphous thermoelectrics. *Phys. Stat. Sol.* **194**, 271–276 (2002).
76. Liang, H. et al. Flexible X-ray detectors based on amorphous Ga_2O_3 thin films. *ACS Photon.* **6**, 351–359 (2019).
77. Clarke, D. R. & Phillpot, S. R. Thermal barrier coating materials. *Mater. Today* **8**, 22–29 (2005).
78. Croissant, J. G., Fatieiev, Y., Almalik, A. & Khashab, N. M. Mesoporous silica and organosilica nanoparticles: physical chemistry, biosafety, delivery strategies, and biomedical applications. *Adv. Healthc. Mater.* **7**, 1700831 (2018).
79. He, S. et al. Semiconductor glass with superior flexibility and high room temperature thermoelectric performance. *Sci. Adv.* **6**, eaaz8423 (2020).

80. Fu, Y. et al. Superflexible inorganic $Ag_2Te_{0.6}S_{0.4}$ fiber with high thermoelectric performance. *Adv. Sci.* **10**, 2207642 (2023).
81. Croissant, J. G., Butler, K. S., Zink, J. I. & Brinker, C. J. Synthetic amorphous silica nanoparticles: toxicity, biomedical and environmental implications. *Nat. Rev. Mater.* **5**, 886–909 (2020).
82. Toh, C.-T. et al. Synthesis and properties of free-standing monolayer amorphous carbon. *Nature* **577**, 199–203 (2020).
83. Tian, H. et al. Disorder-tuned conductivity in amorphous monolayer carbon. *Nature* **615**, 56–61 (2023).
84. Wang, W. H., Dong, C. & Shek, C. H. Bulk metallic glasses. *Mater. Sci. Eng. R. Rep.* **44**, 45–89 (2004).
85. Štich, I., Car, R. & Parrinello, M. Amorphous silicon studied by ab initio molecular dynamics: preparation, structure, and properties. *Phys. Rev. B* **44**, 11092–11104 (1991).
86. McCulloch, D. G., McKenzie, D. R. & Goringe, C. M. Ab initio simulations of the structure of amorphous carbon. *Phys. Rev. B* **61**, 2349–2355 (2000).
87. Akola, J. & Jones, R. O. Structural phase transitions on the nanoscale: the crucial pattern in the phase-change materials $Ge_2Sb_2Te_5$ and GeTe. *Phys. Rev. B* **76**, 235201 (2007).
88. Hegedüs, J. & Elliott, S. R. Microscopic origin of the fast crystallization ability of Ge–Sb–Te phase-change memory materials. *Nat. Mater.* **7**, 399–405 (2008).
89. Aykol, M., Dwaraknath, S. S., Sun, W. & Persson, K. A. Thermodynamic limit for synthesis of metastable inorganic materials. *Sci. Adv.* **4**, eaaq0148 (2018).
90. Behler, J. First principles neural network potentials for reactive simulations of large molecular and condensed systems. *Angew. Chem. Int. Ed.* **56**, 12828–12840 (2017).
91. Deringer, V. L., Caro, M. A. & Csányi, G. Machine learning interatomic potentials as emerging tools for materials science. *Adv. Mater.* **31**, 1902765 (2019).
92. Friederich, P., Häse, F., Proppe, J. & Aspuru-Guzik, A. Machine-learned potentials for next-generation matter simulations. *Nat. Mater.* **20**, 750–761 (2021).
93. Cheng, B., Mazzola, G., Pickard, C. J. & Ceriotti, M. Evidence for supercritical behaviour of high-pressure liquid hydrogen. *Nature* **585**, 217–220 (2020).
94. Muhli, H. et al. Machine learning force fields based on local parametrization of dispersion interactions: application to the phase diagram of C_{60}. *Phys. Rev. B* **104**, 054106 (2021).
95. Zhou, Y., Kirkpatrick, W. & Deringer, V. L. Cluster fragments in amorphous phosphorus and their evolution under pressure. *Adv. Mater.* **34**, 2107515 (2022).
96. Fan, Z. & Tanaka, H. Microscopic mechanisms of pressure-induced amorphous–amorphous transitions and crystallisation in silicon. *Nat. Commun.* **15**, 368 (2024).
97. Zhou, Y., Zhang, W., Ma, E. & Deringer, V. L. Device-scale atomistic modelling of phase-change memory materials. *Nat. Electron.* **6**, 746–754 (2023).
98. Deringer, V. L. & Csányi, G. Machine learning based interatomic potential for amorphous carbon. *Phys. Rev. B* **95**, 094203 (2017).
99. Sosso, G. C., Miceli, G., Caravati, S., Behler, J. & Bernasconi, M. Neural network interatomic potential for the phase change material GeTe. *Phys. Rev. B* **85**, 174103 (2012).
100. Mocanu, F. C. et al. Modeling the phase-change memory material, $Ge_2Sb_2Te_5$, with a machine-learned interatomic potential. *J. Phys. Chem. B* **122**, 8998–9006 (2018).
101. Deringer, V. L. et al. Realistic atomistic structure of amorphous silicon from machine-learning-driven molecular dynamics. *J. Phys. Chem. Lett.* **9**, 2879–2885 (2018).
102. Konstantinou, K., Mocanu, F. C., Lee, T.-H. & Elliott, S. R. Revealing the intrinsic nature of the mid-gap defects in amorphous $Ge_2Sb_2Te_5$. *Nat. Commun.* **10**, 3065 (2019).
103. Simoncelli, M., Mauri, F. & Marzari, N. Thermal conductivity of glasses: first-principles theory and applications. *npj Comput. Mater.* **9**, 106 (2023).
104. Caro, M. A., Deringer, V. L., Koskinen, J., Laurila, T. & Csányi, G. Growth mechanism and origin of high sp^3 content in tetrahedral amorphous carbon. *Phys. Rev. Lett.* **120**, 166101 (2018).
105. Caro, M. A., Csányi, G., Laurila, T. & Deringer, V. L. Machine learning driven simulated deposition of carbon films: from low-density to diamond-like amorphous carbon. *Phys. Rev. B* **102**, 174201 (2020).
106. Choy, K. L. Chemical vapour deposition of coatings. *Prog. Mater. Sci.* **48**, 57–170 (2003).
107. Yang, H.-S. et al. Anomalously high thermal conductivity of amorphous Si deposited by hot-wire chemical vapor deposition. *Phys. Rev. B* **81**, 104203 (2010).
108. Maita, J. M., Song, G., Colby, M. & Lee, S.-W. Atomic arrangement and mechanical properties of chemical-vapor-deposited amorphous boron. *Mater. Des.* **193**, 108856 (2020).
109. Sun, L. et al. Chemical vapour deposition. *Nat. Rev. Methods Primers* **1**, 5 (2021).
110. Wang, H. et al. Efficient screening framework for organic solar cells with deep learning and ensemble learning. *npj Comput. Mater.* **9**, 200 (2023).
111. Basha, B. et al. Designing of novel organic semiconductors materials for organic solar cells: a machine learning assisted proficient pipeline. *Inorg. Chem. Commun.* **153**, 110818 (2023).
112. Yoo, P. et al. Deep learning workflow for the inverse design of molecules with specific optoelectronic properties. *Sci. Rep.* **13**, 20031 (2023).
113. Kilgour, M., Gastellu, N., Hui, D. Y. T., Bengio, Y. & Simine, L. Generating multiscale amorphous molecular structures using deep learning: a study in 2D. *J. Phys. Chem. Lett.* **11**, 8532–8537 (2020).
114. Kwon, H. et al. Spectroscopy-guided discovery of three-dimensional structures of disordered materials with diffusion models. *Mach. Learn. Sci. Technol.* **5**, 045037 (2024).
115. Madanchi, A., Kilgour, M., Zysk, F., Kühne, T. D. & Simine, L. Simulations of disordered matter in 3D with the morphological autoregressive protocol (MAP) and convolutional neural networks. *J. Chem. Phys.* **160**, 024101 (2024).
116. Barkema, G. T. & Mousseau, N. Event-based relaxation of continuous disordered systems. *Phys. Rev. Lett.* **77**, 4358–4361 (1996).
117. Mousseau, N. & Barkema, G. T. Traveling through potential energy landscapes of disordered materials: the activation–relaxation technique. *Phys. Rev. E* **57**, 2419–2424 (1998).
118. Madanchi, A. et al. Is the future of materials amorphous? Challenges and opportunities in simulations of amorphous materials. Preprint at https://arxiv.org/abs/2410.05035 (2024).
119. Opletal, G. et al. Hybrid approach for generating realistic amorphous carbon structure using metropolis and reverse Monte Carlo. *Mol. Simul.* **28**, 927–938 (2002).
120. Nicholas, T. C. et al. Geometrically frustrated interactions drive structural complexity in amorphous calcium carbonate. *Nat. Chem.* **16**, 36–41 (2024).
121. Leist, C., He, M., Liu, X., Kaiser, U. & Qi, H. Deep-learning pipeline for statistical quantification of amorphous two-dimensional materials. *ACS Nano* **16**, 20488–20496 (2022).
122. Zarrouk, T., Ibragimova, R., Bartók, A. P. & Caro, M. A. Experiment-driven atomistic materials modeling: a case study combining X-ray photoelectron spectroscopy and machine learning potentials to infer the structure of oxygen-rich amorphous carbon. *J. Am. Chem. Soc.* **146**, 14645–14659 (2024).
123. Anker, A. S., Butler, K. T., Le, M. D., Perring, T. G. & Thiyagalingam, J. Using generative adversarial networks to match experimental and simulated inelastic neutron scattering data. *Digit. Discov.* **2**, 578–590 (2023).
124. Khan, A., Lee, C.-H., Huang, P. Y. & Clark, B. K. Leveraging generative adversarial networks to create realistic scanning transmission electron microscopy images. *npj Comput. Mater.* **9**, 85 (2023).
125. Sosso, G. C., Donadio, D., Caravati, S., Behler, J. & Bernasconi, M. Thermal transport in phase-change materials from atomistic simulations. *Phys. Rev. B* **86**, 104301 (2012).
126. Aryana, K. et al. Tuning network topology and vibrational mode localization to achieve ultralow thermal conductivity in amorphous chalcogenides. *Nat. Commun.* **12**, 2817 (2021).
127. Liu, Y. et al. Unraveling thermal transport correlated with atomistic structures in amorphous gallium oxide via machine learning combined with experiments. *Adv. Mater.* **35**, 2210873 (2023).
128. Ramprasad, R., Batra, R., Pilania, G., Mannodi-Kanakkithodi, A. & Kim, C. Machine learning in materials informatics: recent applications and prospects. *npj Comput. Mater.* **3**, 54 (2017).
129. Schmidt, J., Marques, M. R. G., Botti, S. & Marques, M. A. L. Recent advances and applications of machine learning in solid-state materials science. *npj Comput. Mater.* **5**, 83 (2019).
130. Raty, J. Y. et al. Aging mechanisms in amorphous phase-change materials. *Nat. Commun.* **6**, 7467 (2015).
131. Behler, J. & Parrinello, M. Generalized neural-network representation of high-dimensional potential-energy surfaces. *Phys. Rev. Lett.* **98**, 146401 (2007).
132. Li, W., Ando, Y., Minamitani, E. & Watanabe, S. Study of Li atom diffusion in amorphous Li_3PO_4 with neural network potential. *J. Chem. Phys.* **147**, 214106 (2017).
133. Chen, C. & Ong, S. P. A universal graph deep learning interatomic potential for the periodic table. *Nat. Comput. Sci.* **2**, 718–728 (2022).
134. Deng, B. et al. CHGNet as a pretrained universal neural network potential for charge-informed atomistic modelling. *Nat. Mach. Intell.* **5**, 1031–1041 (2023).
135. Zheng, H. et al. The ab initio amorphous materials database: empowering machine learning to decode diffusivity. Preprint at https://arxiv.org/abs/2402.00177 (2024).
136. Abou El Kheir, O., Bonati, L., Parrinello, M. & Bernasconi, M. Unraveling the crystallization kinetics of the $Ge_2Sb_2Te_5$ phase change compound with a machine-learned interatomic potential. *npj Comput. Mater.* **10**, 33 (2024).
137. Orava, J., Greer, A. L., Gholipour, B., Hewak, D. W. & Smith, C. E. Characterization of supercooled liquid $Ge_2Sb_2Te_5$ and its crystallization by ultrafast-heating calorimetry. *Nat. Mater.* **11**, 279–283 (2012).
138. Wilson, H. W. On the velocity of solidification and viscosity of super-cooled liquids. *Philos. Mag.* **50**, 238–250 (1900).
139. Niefind, F., Shivhare, R., Mannsfeld, S. C. B., Abel, B. & Hambsch, M. Investigating the morphology of bulk heterojunctions by laser photoemission electron microscopy. *Polym. Test.* **116**, 107791 (2022).
140. Yi, Y., Coropceanu, V. & Brédas, J.-L. Exciton-dissociation and charge-recombination processes in pentacene/C_{60} solar cells: theoretical insight into the impact of interface geometry. *J. Am. Chem. Soc.* **131**, 15777–15783 (2009).
141. Vandervelden, C. A., Khan, S. A., Scott, S. L. & Peters, B. Site-averaged kinetics for catalysts on amorphous supports: an importance learning algorithm. *React. Chem. Eng.* **5**, 77–86 (2019).
142. Zhang, J., Hu, P. & Wang, H. Amorphous catalysis: machine learning driven high-throughput screening of superior active site for hydrogen evolution reaction. *J. Phys. Chem. C* **124**, 10483–10494 (2020).
143. Zhang, D. et al. Unlocking the performance of ternary metal (hydro)oxide amorphous catalysts via data-driven active-site engineering. *Energy Environ. Sci.* **16**, 5065–5075 (2023).
144. Zhang, X., Li, K., Wen, B., Ma, J. & Diao, D. Machine learning accelerated DFT research on platinum-modified amorphous alloy surface catalysts. *Chin. Chem. Lett.* **34**, 107833 (2023).
145. Noh, J. et al. Inverse design of solid-state materials via a continuous representation. *Matter* **1**, 1370–1384 (2019).
146. Ren, Z. et al. An invertible crystallographic representation for general inverse design of inorganic crystals with targeted properties. *Matter* **5**, 314–335 (2022).

147. Ben Mahmoud, C., Gardner, J. L. A. & Deringer, V. L. Data as the next challenge in atomistic machine learning. *Nat. Comput. Sci.* **4**, 384–387 (2024).
148. Jain, A. et al. Commentary: the materials project: a materials genome approach to accelerating materials innovation. *APL Mater.* **1**, 011002 (2013).
149. Zakutayev, A. et al. An open experimental database for exploring inorganic materials. *Sci. Data* **5**, 180053 (2018).
150. Mocanu, F. C., Konstantinou, K. & Elliott, S. R. Quench-rate and size-dependent behaviour in glassy $Ge_2Sb_2Te_5$ models simulated with a machine-learned Gaussian approximation potential. *J. Phys. D Appl. Phys.* **53**, 244002 (2020).
151. Cole, J. M. A design-to-device pipeline for data-driven materials discovery. *Acc. Chem. Res.* **53**, 599–610 (2020).
152. Mikolov, T., Chen, K., Corrado, G. & Dean, J. Efficient estimation of word representations in vector space. Preprint at https://arxiv.org/abs/1301.3781 (2013).
153. Pennington, J., Socher, R. & Manning, C. GloVe: global vectors for word representation. In *Proc. 2014 Conf. Empir. Methods Nat. Lang. Process.* (eds Moschitti, A., Pang, B. & Daelemans, W.) 1532–1543 (Association for Computational Linguistics, 2014).
154. Peters, M. E. et al. Deep contextualized word representations. In *Proc. 2018 Conf. North Am. Chapter Assoc. Comput. Linguist.* (eds Walker, M., Ji, H. & Stent, A.) 2227–2237 (ACL, 2018).
155. Bojanowski, P., Grave, E., Joulin, A. & Mikolov, T. Enriching word vectors with subword information. *Trans. Assoc. Comput. Linguist.* **5**, 135–146 (2017).
156. Tshitoyan, V. et al. Unsupervised word embeddings capture latent knowledge from materials science literature. *Nature* **571**, 95–98 (2019).
157. Devlin, J., Chang, M.-W., Lee, K. & Toutanova, K. BERT: pre-training of deep bidirectional transformers for language understanding. In *Proc. 2019 Conf. North Am. Chapter Assoc. Comput. Linguist.* (eds Burstein, J., Doran, C. & Solorio, T.) 4171–4186 (ACL, 2019).
158. Brown, T. B. et al. Language models are few-shot learners. In *Proc. 34th Int. Conf. Neural Inform. Process. Syst.* (eds Larochelle, H., Ranzato, M., Hadsell, R., Balcan, M. F. & Lin, H.) 1877–1901 (Curran Associates, 2020).
159. Lee, J. et al. BioBERT: a pre-trained biomedical language representation model for biomedical text mining. *Bioinformatics* **36**, 1234–1240 (2020).
160. Court, C. J. & Cole, J. M. Magnetic and superconducting phase diagrams and transition temperatures predicted using text mining and machine learning. *npj Comput. Mater.* **6**, 18 (2020).
161. Kononova, O. et al. Opportunities and challenges of text mining in materials research. *iScience* **24**, 102155 (2021).
162. Gupta, T., Zaki, M., Krishnan, N. M. A. & Mausam MatSciBERT: a materials domain language model for text mining and information extraction. *npj Comput. Mater.* **8**, 102 (2022).
163. Dagdelen, J. et al. Structured information extraction from scientific text with large language models. *Nat. Commun.* **15**, 1418 (2024).
164. Raccuglia, P. et al. Machine-learning-assisted materials discovery using failed experiments. *Nature* **533**, 73–76 (2016).
165. Chang, Y. et al. A survey on evaluation of large language models. *ACM Trans. Intell. Syst. Technol.* **15**, 39:1–39:45 (2024).
166. Sun, W. & David, N. A critical reflection on attempts to machine-learn materials synthesis insights from text-mined literature recipes. *Faraday Discuss.* https://doi.org/10.1039/D4FD00112E (2024).
167. Boström, H. L. B. et al. How reproducible is the synthesis of Zr–porphyrin metal–organic frameworks? An interlaboratory study. *Adv. Mater.* **36**, 2304832 (2024).
168. Shields, B. J. et al. Bayesian reaction optimization as a tool for chemical synthesis. *Nature* **590**, 89–96 (2021).
169. Colliandre, L. & Muller, C. in *High Performance Computing for Drug Discovery and Biomedicine* (ed. Heifetz, A.) 101–136 (Springer, 2024).
170. Häse, F., Roch, L. M., Kreisbeck, C. & Aspuru-Guzik, A. Phoenics: a Bayesian optimizer for chemistry. *ACS Cent. Sci.* **4**, 1134–1145 (2018).
171. Braconi, E. & Godineau, E. Bayesian optimization as a sustainable strategy for early-stage process development? A case study of Cu-catalyzed C–N coupling of sterically hindered pyrazines. *ACS Sustain. Chem. Eng.* **11**, 10545–10554 (2023).
172. Liu, C. et al. Understanding causalities in organic photovoltaics device degradation in a machine-learning-driven high-throughput platform. *Adv. Mater.* **36**, 2300259 (2024).
173. Coli, G. M., Boattini, E., Filion, L. & Dijkstra, M. Inverse design of soft materials via a deep learning-based evolutionary strategy. *Sci. Adv.* **8**, eabj6731 (2022).
174. Zhou, Z., Li, X. & Zare, R. N. Optimizing chemical reactions with deep reinforcement learning. *ACS Cent. Sci.* **3**, 1337–1344 (2017).
175. Sanchez-Lengeling, B. & Aspuru-Guzik, A. Inverse molecular design using machine learning: generative models for matter engineering. *Science* **361**, 360–365 (2018).
176. Valleti, M., Vasudevan, R. K., Ziatdinov, M. A. & Kalinin, S. V. Bayesian optimization in continuous spaces via virtual process embeddings. *Digit. Discov.* **1**, 910–925 (2022).
177. Anker, A. S. et al. Characterising the atomic structure of mono-metallic nanoparticles from X-ray scattering data using conditional generative models. Preprint at https://chemrxiv.org/abs/12662222.v1 (2020).
178. Kjær, E. T. S. et al. DeepStruc: towards structure solution from pair distribution function data using deep generative models. *Digit. Discov.* **2**, 69–80 (2023).
179. Anstine, D. M. & Isayev, O. Generative models as an emerging paradigm in the chemical sciences. *J. Am. Chem. Soc.* **145**, 8736–8750 (2023).
180. Groom, C. R., Bruno, I. J., Lightfoot, M. P. & Ward, S. C. The Cambridge structural database. *Acta Crystallogr. B Struct. Sci. Cryst. Eng. Mater.* **72**, 171–179 (2016).
181. Belsky, A., Hellenbrandt, M., Karen, V. L. & Luksch, P. New developments in the Inorganic Crystal Structure Database (ICSD): accessibility in support of materials research and design. *Acta Crystallogr. B* **58**, 364–369 (2002).
182. Zunger, A., Wei, S.-H., Ferreira, L. G. & Bernard, J. E. Special quasirandom structures. *Phys. Rev. Lett.* **65**, 353–356 (1990).
183. Thyagarajan, R. & Sholl, D. S. A database of porous rigid amorphous materials. *Chem. Mater.* **32**, 8020–8033 (2020).
184. Cheng, J., Fong, K. D. & Persson, K. A. Materials design principles of amorphous cathode coatings for lithium-ion battery applications. *J. Mater. Chem. A* **10**, 22245–22256 (2022).
185. Batatia, I. et al. A foundation model for atomistic materials chemistry. Preprint at https://arxiv.org/abs/2401.00096 (2023).
186. Zhang, D. et al. DPA-2: a large atomic model as a multi-task learner. Preprint at https://arxiv.org/abs/2312.15492 (2024).
187. Gardner, J. L. A., Baker, K. T. & Deringer, V. L. Synthetic pre-training for neural-network interatomic potentials. *Mach. Learn. Sci. Technol.* **5**, 015003 (2024).
188. Kaur, H. et al. Data-efficient fine-tuning of foundational models for first-principles quality sublimation enthalpies. *Faraday Discuss.* https://doi.org/10.1039/D4FD00107A (2024).
189. Lunt, A. M. et al. Modular, multi-robot integration of laboratories: an autonomous workflow for solid-state chemistry. *Chem. Sci.* **15**, 2456–2463 (2024).
190. Pithan, L. et al. Closing the loop: autonomous experiments enabled by machine-learning-based online data analysis in synchrotron beamline environments. *J. Synchrotron Radiat.* **30**, 1064–1075 (2023).
191. Huang, J.-X., Csányi, G., Zhao, J.-B., Cheng, J. & Deringer, V. L. First-principles study of alkali-metal intercalation in disordered carbon anode materials. *J. Mater. Chem. A* **7**, 19070–19080 (2019).
192. Deringer, V. L. et al. Towards an atomistic understanding of disordered carbon electrode materials. *Chem. Commun.* **54**, 5988–5991 (2018).
193. Ke, G. et al. LightGBM: a highly efficient gradient boosting decision tree. In *31st Conf. Advances Neural Inform. Process. Syst.* (eds Guyon, I. et al.) (Curran Associates, 2017).
194. El-Machachi, Z. et al. Accelerated first-principles exploration of structure and reactivity in graphene oxide. *Angew. Chem. Int. Ed.* https://doi.org/10.1002/anie.202410088 (2024).
195. Spöri, C., Kwan, J. T. H., Bonakdarpour, A., Wilkinson, D. P. & Strasser, P. The stability challenges of oxygen evolving catalysts: towards a common fundamental understanding and mitigation of catalyst degradation. *Angew. Chem. Int. Ed.* **56**, 5994–6021 (2017).
196. Wu, G. et al. A general synthesis approach for amorphous noble metal nanosheets. *Nat. Commun.* **10**, 4855 (2019).
197. Cheng, H., Yang, N., Lu, Q., Zhang, Z. & Zhang, H. Syntheses and properties of metal nanomaterials with novel crystal phases. *Adv. Mater.* **30**, 1707189 (2018).
198. Griffin, J. M. et al. In situ NMR and electrochemical quartz crystal microbalance techniques reveal the structure of the electrical double layer in supercapacitors. *Nat. Mater.* **14**, 812–819 (2015).
199. Pecher, O., Carretero-González, J., Griffith, K. J. & Grey, C. P. Materials' methods: NMR in battery research. *Chem. Mater.* **29**, 213–242 (2017).
200. Cao, C., Li, Z.-B., Wang, X.-L., Zhao, X.-B. & Han, W.-Q. Recent advances in inorganic solid electrolytes for lithium batteries. *Front. Energy Res.* **2**, 388–416 (2014).
201. Xu, Z. & Xia, Y. Progress, challenges and perspectives of computational studies on glassy superionic conductors for solid-state batteries. *J. Mater. Chem. A* **10**, 11854–11880 (2022).
202. Schulmeister, K. & Mader, W. TEM investigation on the structure of amorphous silicon monoxide. *J. Non Cryst. Solids* **320**, 143–150 (2003).
203. Hirata, A. et al. Atomic-scale disproportionation in amorphous silicon monoxide. *Nat. Commun.* **7**, 11591 (2016).
204. Heremans, P. et al. Mechanical and electronic properties of thin-film transistors on plastic, and their integration in flexible electronic applications. *Adv. Mater.* **28**, 4266–4282 (2016).
205. Liu, L. & Zhang, C. Fe-based amorphous coatings: structures and properties. *Thin Solid Films* **561**, 70–86 (2014).
206. Calin, M. et al. Designing biocompatible Ti-based metallic glasses for implant applications. *Mater. Sci. Eng. C* **33**, 875–883 (2013).
207. Zhong, L., Wang, J., Sheng, H., Zhang, Z. & Mao, S. X. Formation of monatomic metallic glasses through ultrafast liquid quenching. *Nature* **512**, 177–180 (2014).
208. Sohrabi, N., Jhabvala, J. & Logé, R. E. Additive manufacturing of bulk metallic glasses — process, challenges and properties: a review. *Metals* **11**, 1279 (2021).
209. Cheng, H. et al. Ligand-exchange-induced amorphization of Pd nanomaterials for highly efficient electrocatalytic hydrogen evolution reaction. *Adv. Mater.* **32**, 1902964 (2020).
210. Billinge, S. J. L. & Levin, I. The problem with determining atomic structure at the nanoscale. *Science* **316**, 561–565 (2007).
211. Momma, K. & Izumi, F. VESTA 3 for three-dimensional visualization of crystal, volumetric and morphology data. *J. Appl. Crystallogr.* **44**, 1272–1276 (2011).
212. Stukowski, A. Visualization and analysis of atomistic simulation data with OVITO — the open visualization tool. *Model. Simul. Mater. Sci. Eng.* **18**, 015012 (2010).

Acknowledgements

This work was supported by UK Research and Innovation (grant number EP/X016188/1). The work presented in this article is supported by Novo Nordisk Foundation grant number NNF23OC0081359. Structures were visualized with the help of VESTA[211] and OVITO[212].

Author contributions
Y.L. and V.L.D. prepared the initial draft. All authors contributed to the writing of the paper.

Competing interests
The authors declare no competing interests.

Additional information
Peer review information *Nature Reviews Materials* thanks Kedar Hippalgaonkar, Kiran Prasai and the other, anonymous, reviewer(s) for their contribution to the peer review of this work.